

# ESO Phase 3 Data Release Description

Data Collection	KiDS
Release Number	5.0
Data Provider	Konrad Kuijken
Date	17.03.2025

## [ESO Phase 3 Data Release Description](#)

[Abstract](#)

[Overview of Observations](#)

[Imaging products and single-band source lists](#)

[10-band source catalogue](#)

[Data Reduction, Calibration and Photometry](#)

[DR5 fits files and format](#)

[Format of coadded images](#)

[Catalogue Columns](#)

[Acknowledgements](#)

## Abstract

This data release constitutes the fifth public release by the Kilo-Degree Survey (KiDS). KiDS is an ESO public survey carried out with the VLT Survey Telescope and OmegaCAM camera, that has imaged 1347 square degrees in four filters (u, g, r, i). Single epoch observations are provided in (u,g,r). Multi-epoch imaging is provided in the i-band, with the two observations, denoted  $i_1$  and  $i_2$ , typically separated by several years. KiDS was designed as a weak lensing tomography survey, with a core science driver to map and constrain the properties of the evolving large-scale matter distribution in the Universe. The median r-band  $5\sigma$  limiting magnitude is 24.8 with median seeing 0.7". Additional science cases are manifold, ranging from galaxy evolution to Milky Way structure, and from the detection of white dwarfs to high-redshift quasars.

This document summarises the KiDS-ESO-DR5 release, which builds from the fourth KiDS data release with a 34% areal extension as well as a second pass over the full survey area in the i band (effectively doubling the i band integration time for every tile). For each of the 1347 square-degree survey tiles, the data release includes calibrated stacked images in u,g,r,  $i_1$  and  $i_2$  filters, their corresponding weights and masks, and single-band source lists extracted from the stacks. A multi-band  $ugri_1i_2ZYJHK_s$  source catalogue incorporating near-IR photometry from the companion VIKING survey with VISTA is also provided. This catalogue encompasses the combined 1347 square degree area of this data release, with PSF-homogenised and

aperture-matched photometry, and derived photometric redshift and stellar mass estimates. We refer the reader to [Wright et al 2024](#) (hereafter [W24](#)) for a detailed discussion of this data release.

The VST data included in KiDS-ESO-DR5 were taken under ESO programme IDs: 60.A-9038(A), 0103.A-0181(A), 177.A-3016(A to U), 177.A-3016(W), 177.A-3017(A) and 177.A-3018(A). The VISTA data used in this data release are taken from VIKING DR4, released on March 17, 2020.

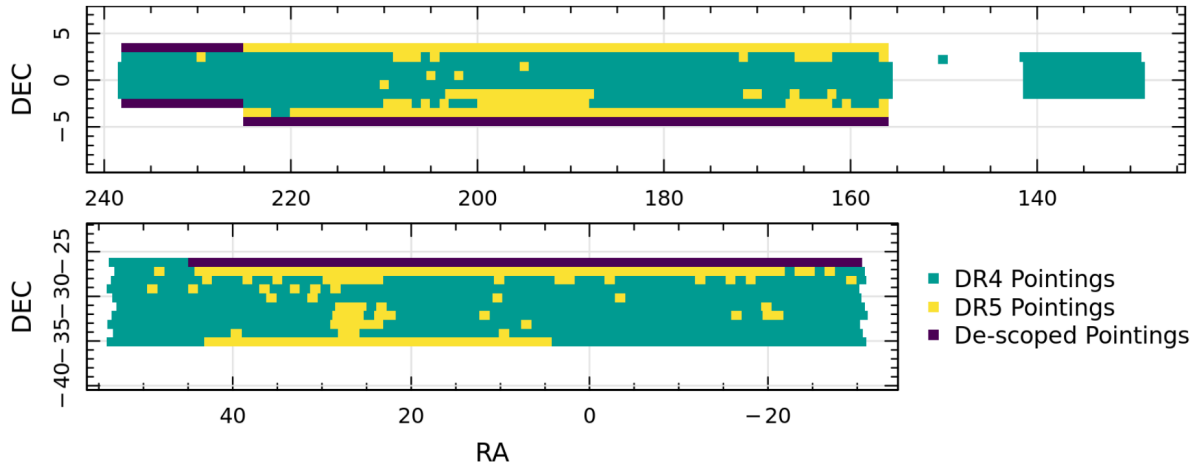


*Figure 1: Location of the 1347 KiDS-ESO-DR5 tiles. The area covered in DR4 is shown in green, while the yellow tiles are new additions. Pointings that were originally included in the 1500 deg<sup>2</sup> KiDS footprint, but which were subsequently descoped due to the limited area observed by VIKING, are shown in dark purple (top: KiDS-North; bottom: KiDS-South).*

Full resolution Hierarchical Progressive Surveys (HiPS) zoomable colour images of the KiDS-ESO-DR5 VST data can be viewed at the following addresses:

[https://alasky.cds.unistra.fr/KiDS/CDS\\_P\\_KiDS\\_DR5\\_color-gri/](https://alasky.cds.unistra.fr/KiDS/CDS_P_KiDS_DR5_color-gri/) (g/r/i), and

[https://alasky.cds.unistra.fr/KiDS/CDS\\_P\\_KiDS\\_DR5\\_color-ug/](https://alasky.cds.unistra.fr/KiDS/CDS_P_KiDS_DR5_color-ug/) (u/u+g/g),

as well as in the Aladin sky viewer and other HiPS-aware clients.

## Overview of Observations

The KiDS-ESO-DR5 data release consists of the co-added images, weight maps, masks and source lists for 1347 square degree survey tiles observed with OmegaCAM on the VST in u, g, r and i bands between August 9, 2011 and May 3, 2019 (see the DR5 footprint in Figure 1). In addition we release a 10-band  $ugri_1i_2ZYJHK_s$  source catalogue. The DR5 data products supersede all previous KiDS releases.

DR5 provides an additional 341 survey tiles to the KiDS DR4 footprint, along with a full second i-band pass of the full footprint. These tiles have been processed in a similar way to DR4, adopting the same masking, astrometric calibration and photometric calibration algorithms. DR5 updates relative to the previous DR4 release are as follows

- The masking algorithm for the r-band was improved (see section 3.5.3 of W24).
- We reviewed the u-band DR4 astrometric distortion solution, noting that the paucity of stars (per chip) in the u-band can occasionally lead to a poorly constrained 3rd order polynomial fit. This led to unphysical distortion solutions for some chips. For DR5, u-band exposures with more than a 1 arcsecond chip-corner distortion residual have therefore been re-processed using a linear order polynomial fit. This impacts 307 tiles, as listed in Table D1 of W24.
- The photometric calibration, using stellar locus regression, was updated to include the new  $i_2$  photometry (see section 3.5.2 of W24). Any DR4 data products that were otherwise unchanged by our DR5 re-analysis have only been updated with this revised zero-point calibration information.

The new DR5 10-band  $ugri_{i_2}ZYJHK_s$  source catalogue spans all survey tiles in the data release. It contains list-driven, aperture- and PSF-matched [GAAP photometry](#) (Kuijken et al 2015) from the stacked VST images, and VISTA images taken as part of the near-IR VIKING survey. Derived parameters include star-galaxy classifiers, photometric redshifts from the [BPZ algorithm](#) (Benitez 2000) and stellar mass estimates from the [LePhare](#) algorithm (Arnouts et al 1999). Sources are detected on a separate reduction of the r-band stacks with the [THELI](#) pipeline (Erben et al 2005), optimised for the weak lensing analysis. These r-band detection images are also included in the data release, superseding their DR4 equivalent owing to the use of an improved Gaia-based astrometric solution.

## Imaging products and single-band source lists

A list of the 1347 tiles for which imaging data products and single-band source lists are provided for [KiDS-ESO-DR5](#) is online.

Each tile was observed in the u, g, r, and i band. The final footprint of each tile is slightly larger than 1 square degree due to the dithering scheme: 61.9x65.4 arcminutes in u; 62.3x66.8 arcminutes in g, r and i. The total unique sky coverage of the KiDS footprint is 1331 square degrees, which reduces to 1014 square degrees when applying the KiDS-recommended masks in both the VST and VIKING filters (see Table 12 of W24).

As the OmegaCAM CCD mosaic consists of 32 individual CCDs, the sky covered by a single exposure has gaps. In order to fill in these gaps, KiDS tiles are built up from 5 dithered observations in g, r and i and 4 in u. The dithers form a staircase pattern with dither steps of 25" in X (RA) and 85" in Y (DEC), bridging the inter-CCD gaps (see Figure 3 of [de Jong et al., 2015](#)). The tile centres are based on a tiling strategy that tiles the full sky efficiently for

VST/OmegaCAM. Neighbouring dithered stacks have an overlap in RA of 5% and in DEC of 10%.

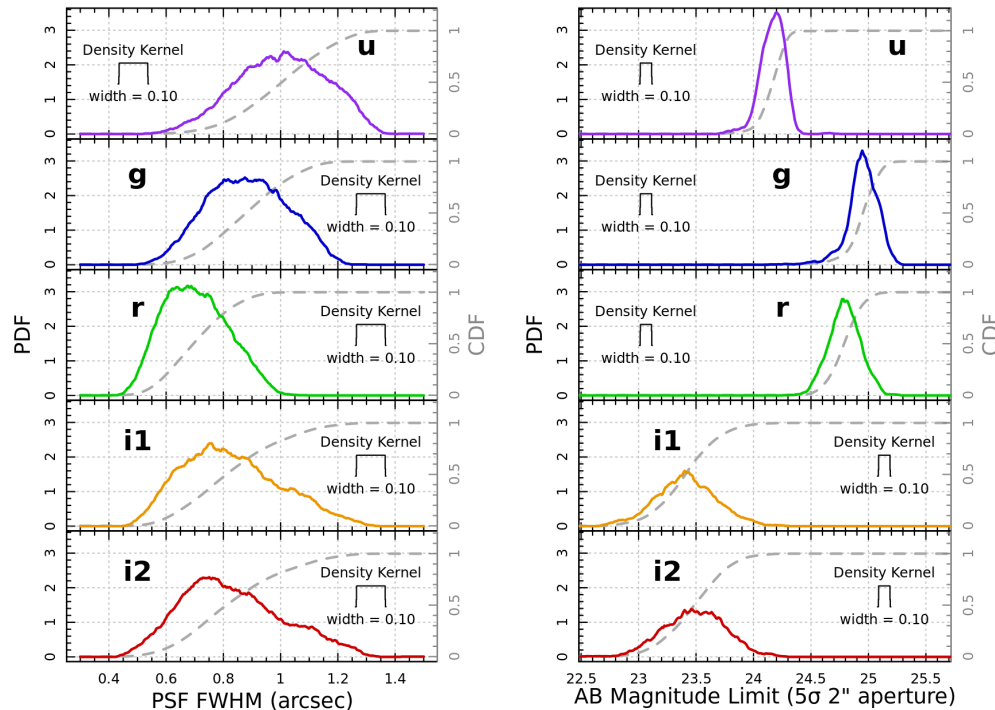


Figure 2: Tile-by-tile raw data quality parameters for KiDS-ESO-DR5. Left: average PSF size (FWHM) distributions; right: limiting magnitude distributions ( $5\sigma$  AB in  $2''$  aperture). The distributions are per filter: from top to bottom u, g, r, and then the multi-epoch i1 and i2 bands. See Section 3.1.3 of W24 for details.

In Figure 2 the obtained seeing (FWHM), and limiting magnitude ( $5\sigma$  AB in  $2''$  aperture) distributions per filter are shown, to illustrate the obtained data quality. In the case of filters observed during dark time (u, g, r), the FWHM distributions reflect the different observing constraints, with r-band taking the best conditions. As the i-band is the only filter observed in bright time, we recover a large range of seeing conditions in this filter. The wide range of i-band limiting magnitudes is caused by the larger range in seeing and moon phase and thus sky brightness. We note that the second-pass i-band imaging does not suffer from the poor baffling of the VST in the period up to May 2015 that particularly affected the i-band sky background.

The VST-PSF is quite round and shows little variation across the focal plane: seeing ellipticities (defined as  $e = 1 - b/a$ , where a and b are the major and minor axes of the PSF, respectively) across all KiDS VST observations are consistently less than  $\langle e \rangle = 0.08$  per exposure (see Appendix G of W24 for details).

The flux scales in the images correspond to the nightly zeropoints, with the post-processing calibration zeropoints reported in the image header. The single-band source lists were extracted from the calibrated, stacked images for each tile and filter separately, using the Astro-WISE processing system (see Section 3.5.5 in W24). These catalogues are provided to

the public largely ‘as-is’; they have not gone through the same rigorous quality control and testing as the 10-band catalogues discussed in the next section.

For a full overview of the data quality parameters for each observation we refer to the following online table: [http://kids.strw.leidenuniv.nl/DR5/data\\_table.php](http://kids.strw.leidenuniv.nl/DR5/data_table.php). This data release consists of 26,940 files of single-band data, totalling 20.8TB (image, weight, mask and source list).

## 10-band source catalogue

The KiDS-ESO-DR5  $ugri_{i_2}ZYJHK_s$  source catalogue combines VST and VISTA observations over the complete KiDS footprint.

The detection catalogue was generated from the r-band images reduced with the THELI pipeline described in section 3.2 of W24. These images form the basis for weak lensing shape measurements, and this choice ensures that the definition of the sources in the photometric catalogue is consistent with the lensing catalogue. The complementary shear catalogue will be released on the KiDS website after the publication of the DR5 cosmic shear analysis (see Wright et al 2025 and Stolzner et al 2025).

Photometric calibration for the 10-band source catalogue uses stellar-locus regression, anchored to a combination of Gaia photometry (in the white-light G-band, blue GBP-band, and red GRP-band). Section 3.5.2 of W24 describes the calibration process, and how the second i-band pass is used to estimate the systematic uncertainty introduced in the calibration of the ugr-bands by variations in the quality of the i-band data. The KiDS reduction and calibration of the NIR VIKING imaging is described in Section 4 of W24.

We report forced (list-driven) ‘Gaussian Aperture and PSF (GAaP)’ photometry ([Kuijken et al. 2015](#)) on the Astro-WISE ugr<sub>1</sub>VST images, and the ZYJHK<sub>s</sub> VISTA images. For details see section 3.6 of W24. GAaP photometry requires the same aperture to be specified across all bands, and this aperture must not be smaller than the seeing. To accommodate occasional poor seeing in one of the 10 bands, GAaP photometry is recorded for two choices of a minimum Gaussian aperture rms radius: 0.7” and 1.0”. When the seeing is good in all bands the smaller setting will yield the most accurate measurements, but for a band where the seeing is poor, the larger aperture may yield a more accurate flux, or the smaller aperture may not yield a flux measurement at all. The optimal choice of aperture radius is made source by source.

During our weak lensing analysis we discovered systematic failures in the DR5 astrometric solution used in the THELI calibration of r-band images. These were identified from the measurement of two statistics

1. The difference between the centroids of all sources extracted from AstroWISE and THELI co-added images, matched within 2” and computed in 1’x1’ bins on sky (`max_dRADec_AW`)

2. The difference between the centroids of point-like high signal-to-noise objects extracted from individual THELI exposures, also matched within 2" and computed in 1'x1' bins on sky (max\_dRADec\_THELI)

Using the measurement of B-modes in the cosmic shear signal as a metric of systematic contamination from these astrometric errors, we empirically determined criteria to remove problematic regions in our images. The catalogues include `ast_flag`, which is set to 1 if the object is safe to use with  $\text{max\_dRADec\_AW} \leq 0.06/3600$  and  $\text{max\_dRADec\_THELI} \leq 0.2/3600$ . This selection rejects 46.6 square degrees of data from the masked KiDS-DR5 footprint. If your analysis of the KiDS-DR5 10-band catalogue requires very accurate astrometry and photometry, we recommend either using `ast_flag` in your object selection, or optimising your own criteria using the centroid-differences that are provided. Healpix masks of the DR5 footprint that include the `ast_flag` effective selection mask are available from the KiDS website.

The 10-band catalogue contains a total of 138,812,117 unique sources, with accurate photometry measurements in all 10 bands for a subset of 100,197,893. The catalogue constitutes 1348 files (1347 data files and 1 metadata file), and has a total data volume of 212 GB. An additional 4041 THELI data products (totalling 4.1TB) are also provided (image, weight, 10-band mask).

## Data Reduction, Calibration and Photometry

The KiDS-ESO data reduction and calibration pipeline is detailed in this series of papers

- The Astro-WISE optical pipeline: [McFarland et al. \(2013, ExA 35, 45\)](#)
- KiDS-ESO-DR1/2: [de Jong et al. 2015, A&A, 582, A62](#)
- KiDS-ESO-DR3: [de Jong et al, 2017, A&A, 604, A134](#)
- KiDS-VIKING: [Wright et al. 2019, A&A, 632, A34](#)
- KiDS-ESO-DR4: [Kuijken et al. 2019, A&A, 625, A2](#)
- KiDS-ESO-DR5: [Wright et al 2024 \(W24\)](#)

Section 3.5 of W24 documents the DR5-specific changes in the Astro-WISE reduction and calibration relative to DR4: an improved astrometric solution for 307 u-band co-adds, newly derived cross-talk coefficients for the later DR5 observations, calibration updates to account for the second i-band pass, improved r-band masks and the addition of careful manual masking for a handful of problematic fields. The DR5 data products supersede all previous KiDS releases.

For detailed information about the data reduction and calibration we refer the user to the publications listed above. This reference table is designed to help you quickly find the information you seek.

Topic	Location
Survey area for different mask values	W24 Table 12
10-band area, magnitude limits, exposure times	W24 Table 1
Image de-trending	<a href="#">de Jong et al 2015</a> , Section 4.1
DR5 Cross-talk coefficients	W24 Table 5
Astrometry	W24 Sect 3.2.1, Figs 8-12 and Appendix C
Automated Masks	W24 Sect 3.5.3, Fig 16 <a href="#">de Jong et al 2015</a> , Sect 4.4
Manual Masks	W24 Sect 3.5.5, Fig 17
VST Baffle configurations: pre May 2015 data can suffer from scattered light and reflections	<a href="#">de Jong et al 2017</a> , Table 4
SExtractor source extraction parameters	W24 Table 4
GAAp photometry algorithm	W24 Sect 3.6 and <a href="#">Kuijken et al 2019</a> , Sect 3.1.1
Optimal GAAp photometry (0p7 or 1p0 flux)	<a href="#">Kuijken et al 2019</a> , Sect 5, equations 9&10 & W24 Sect 6.2
Zero-point calibration: stellar locus regression with SDSS DR16 and Gaia eDR3.	W24 Sect 3.5.2, Fig 13,15
10-band Mask bit values for the different filters	W24 Table 11
Single Band Source Catalogues	<a href="#">Kuijken et al 2019</a> Table A.3
Single Band Star/Gal classification via the 2DPHOT flag	<a href="#">de Jong et al 2015</a> , Sect 4.5.1
NIR Photometry comparison to 2MASS	<a href="#">Wright et al 2019</a> , Figure 4
Data Quality as a function of ra/dec	W24 Appendix B&E
Photometric Redshift estimation and quality	W24 Sect 6.3, Figure 25 & 26
Stellar Mass estimation	<a href="#">Wright et al 2019</a> , Sect 4.3



## DR5 fits files and format

The naming convention used for all new data products is the following:

KiDS\_DR5.0\_R.R\_D.D\_F\_TTT.fits,

where R.R and D.D are the RA and DEC of the tile centre in degrees (J2000.0) with 1 decimal place, F is the filter (u, g, r, i1, i2 for single-band data files, “ugri1i2ZYJHKs” for multi-band catalogue files), and TTT is the data product type (see column 4 of the Table below). For example: the u-band stacked image of the tile “KiDS\_44.4\_-29.2” is called KiDS\_DR5.0\_44.4\_-29.2\_u\_sci.fits.

Data product	ESO product category name	File type	TTT	F
Calibrated, stacked images	SCIENCE.IMAGE	FITS image	sci	u,g,r,i1,i2
Weight frames	ANCILLARY.WEIGHTMAP	FITS image	wei	u,g,r,i1,i2
Masks	ANCILLARY.MASK	FITS image	msk	u,g,r,i1,i2
Single-band source lists	SCIENCE.SRCTBL	Binary FITS table	src	u,g,r,i1,i2
Multi-band catalogue data file	SCIENCE.MCATALOG	Binary FITS table	cat	ugri1,i2ZYJHKs
THELI detection image	ANCILLARY.IMAGE	FITS image	det_sci	r
THELI weight image	ANCILLARY.IMAGE	FITS image	det_wei	r
Multi-band mask image	ANCILLARY.MASK	FITS image	msk	ugri1,i2ZYJHKs

## Format of coadded images

The final calibrated, coadded images from the Astro-WISE pipeline have a uniform pixel scale of 0.2 arcsec. The pixel units are fluxes relative to the flux corresponding to magnitude = 0, as based on nightly photometric calibrations. This means that the effective zero-point is equal to 0 and the magnitude  $m$  corresponding to a pixel value  $f$  is:

$$m = -2.5 \log_{10} f.$$

Subsequent photometric zeropoint corrections were derived from the catalogues and recorded in the image headers using the DMAG keyword, with the CALSTARS keyword recording the number of Gaia stars that were used in the calibration. For DR5, we calculate calibration values relative to both the  $i_1$  and the new  $i_2$  epoch image. We also use two photometric apertures, setting the GAAP MINAPER parameter to both 0.7 and 1.0 (see Appendix A.1.1 of [Kuijken et al](#)



[2019](#) for details). This results in the following set of keywords reported in the image and source list headers:

- DMAG\_07\_i1
- DMAG\_10\_i1
- DMAG\_07\_i2
- DMAG\_10\_i2
- CALSTARS\_07\_i1
- CALSTARS\_10\_i1
- CALSTARS\_07\_i2
- CALSTARS\_10\_i2

along with:

- DMAG
- CALSTARS

which are the “best” values to use (depending on the PSF size, so either 0.7 or 1.0 aperture as recorded with the CALMINAO keyword), and taking the average of i1 and i2.

The r-band detection images, which result from a reduction using THELI, specifically designed for optimal image shape measurement and small astrometric reductions, are the basis of the multi-band catalogue. They have a pixel scale that is closer to the native OmegaCAM pixel size of 0.213”.

## Catalogue Columns

For a description and catalogue column list we refer the reader to:

- Single-band source lists: Table A.3 of [Kuijken et al 2019](#)
- Multi-band catalogue: Table I.1 of [W24](#) which we also repeat below for completeness.

Each detected source has been assigned an ID of the form e.g *KiDSDR5*

*J112250.874-005830.69* where the number encodes the RA and Dec as:

$J\{\text{ra\_hour:2}\}\{\text{ra\_min:2}\}\{\text{ra\_sec:2.3}\}\{\text{dec\_sign}\}\{\text{dec\_degree:2}\}\{\text{dec\_min:2}\}\{\text{dec\_sec:2.2}\}$ .

The example ID *KiDSDR5 J112250.874-005830.69* is at RA 11h 22m 50.874s and Dec -00 58m 30.69s

With improvements in our astrometric solution for both KiDS-DR4 and KiDS-DR5, a source that is detected in each data release, will have a slightly different ID.

- Sources detected in the first three data releases use the source identifier KiDS.
- Sources detected in the fourth data release use the source identifier KiDSDR4.
- Sources detected in the fifth data release use the source identifier KiDSDR5.

We recommend catalogue users update their KiDS data to use only sources with the KiDSDR5 identifier as this supersedes all previous releases.

Label	Unit	Format	Description
<b>Identifiers per source and Pointing on-sky:</b>			
ID		30A	ESO ID
KIDS_TILE		16A	Name of the pointing in Astro-WISE convention
THELI_NAME		16A	Name of the pointing in THELI convention
SeqNr		1J	Running object number within the catalogue
SLID		1J	Astro-WISE Source list ID
SID		1J	Astro-WISE Source ID within the source list
<b>Parameters derived from the THELI r-band detection image:</b>			
FLUX_AUTO	Jy	1E	r-band flux
FLUXERR_AUTO	Jy	1E	Error on FLUX_AUTO
MAG_AUTO	mag	1E	r-band magnitude
MAGERR_AUTO	mag	1E	Error on MAG_AUTO
KRON_RADIUS	pixel	1E	Scaling radius of the ellipse for magnitude measurements
BackGr	Jy	1E	Background counts at centroid position
Level	Jy	1E	Detection threshold above background
MU_THRESHOLD	mag.arcsec <sup>-2</sup>	1E	Detection threshold above background
MaxVal	Jy	1E	Peak flux above background
mag.arcsec <sup>-2</sup>	mag.arcsec <sup>-2</sup>	1E	Peak surface brightness above background
ISOAREA_WORLD	deg <sup>2</sup>	1E	Isophotal area above analysis threshold
Xpos	pixel	1E	Centroid x position in the THELI image
Ypos	pixel	1E	Centroid y position in the THELI image
RAJ2000	deg	1D	Centroid sky position right ascension (J2000)
DECJ2000	deg	1D	Centroid sky position declination (J2000)
A_WORLD	deg	1E	Profile RMS along major axis
B_WORLD	deg	1E	Profile RMS along minor axis
THETA_J2000	deg	1E	Position angle (West of North)
THETA_WORLD	deg	1E	Position angle (Counterclockwise from world x-axis)
ERRA_WORLD	deg	1E	World RMS position error along major axis
ERRB_WORLD	deg	1E	World RMS position error along minor axis
ERRTHETA_J2000	deg	1E	Error on THETA_J2000
ERRTHETA_WORLD	deg	1E	Error on THETA_WORLD
FWHM_IMAGE	pixel	1E	FWHM assuming a Gaussian object profile
FWHM_WORLD	deg	1E	FWHM assuming a Gaussian object profile
Flag		1I	SExtractor extraction flags
FLUX_RADIUS	pixel	1E	Half-light radius
CLASS_STAR		1E	Star-galaxy classifier
MAG_ISO	mag	1E	r-band isophotal Magnitude
MAGERR_ISO	mag	1E	Error on MAG_ISO
FLUX_ISO	Jy	1E	r-band isophotal Flux
FLUXERR_ISO	Jy	1E	Error on FLUX_ISO
MAG_ISOCOR	mag	1E	r-band corrected Isophotal Magnitude
MAGERR_ISOCOR	mag	1E	Error on MAG_ISOCOR

FLUX_ISOCOR	Jy	1E	r-band corrected Isophotal Flux
FLUXERR_ISOCOR	Jy	1E	Error on FLUX_ISOCOR
NIMAFLAGS_ISO		1I	Number of flagged pixels over the isophotal profile
IMAFLAGS_ISO		1I	FLAG-image flags ORed over the isophotal profile
XMIN_IMAGE	pixel	1I	Minimum x-coordinate among detected pixels
YMIN_IMAGE	pixel	1I	Minimum y-coordinate among detected pixels
XMAX_IMAGE	pixel	1I	Maximum x-coordinate among detected pixels
YMAX_IMAGE	pixel	1I	Maximum y-coordinate among detected pixels
X_WORLD	deg	1D	Barycentre position along world x axis
Y_WORLD	deg	1D	Barycentre position along world y axis
X2_WORLD	deg <sup>2</sup>	1E	Variance of position along X_WORLD (alpha)
Y2_WORLD	deg <sup>2</sup>	1E	Variance of position along Y_WORLD (delta)
XY_WORLD	deg <sup>2</sup>	1E	Covariance of position X_WORLD,Y_WORLD
ERRX2_WORLD	deg <sup>2</sup>	1E	Error on X2_WORLD
ERRY2_WORLD	deg <sup>2</sup>	1E	Error on Y2_WORLD
ERRXY_WORLD	deg <sup>2</sup>	1E	Error on XY_WORLD
CXX_WORLD	deg <sup>-2</sup>	1E	SExtractor Cxx object ellipse parameter
CYY_WORLD	deg <sup>-2</sup>	1E	SExtractor Cyy object ellipse parameter
CXY_WORLD	deg <sup>-2</sup>	1E	SExtractor Cxy object ellipse parameter
ERRCXX_WORLD	deg <sup>-2</sup>	1E	Error on CXX_WORLD
ERRCYY_WORLD	deg <sup>-2</sup>	1E	Error on CYY_WORLD
ERRCXY_WORLD	deg <sup>-2</sup>	1E	Error on CXY_WORLD
A_IMAGE	pixel	1D	Profile RMS along x-axis
B_IMAGE	pixel	1D	Profile RMS along y-axis
ERRA_IMAGE	pixel	1E	Error on A_IMAGE
ERRB_IMAGE	pixel	1E	Error on B_IMAGE
S_ELLIPTICITY		1E	SExtractor ellipticity (1-B_IMAGE/A_IMAGE)
S_ELONGATION		1E	SExtractor elongation (A_IMAGE/B_IMAGE)
MAG_APER_4	mag	1E	r-band magnitude within a circular aperture of 4 pixels
MAGERR_APER_4	mag	1E	Error on MAG_APER_4
FLUX_APER_4	Jy	1E	r-band flux within a circular aperture of 4 pixels
FLUXERR_APER_4	Jy	1E	Error on FLUX_APER_4
<i>Similarly for radii 6, 8, 10, 14, 20, 30, 40, 60</i>			
MAG_APER_100	mag	1E	r-band magnitude within a circular aperture of 100 pixels
MAGERR_APER_100	mag	1E	Error on MAG_APER_100
FLUX_APER_100	Jy	1E	r-band flux within a circular aperture of 100 pixels
FLUXERR_APER_100	Jy	1E	Error on FLUX_APER_100
ISO0	pixel <sup>2</sup>	1I	Isophotal area at level 0
ISO1	pixel <sup>2</sup>	1I	Isophotal area at level 1
ISO2	pixel <sup>2</sup>	1I	Isophotal area at level 2
ISO3	pixel <sup>2</sup>	1I	Isophotal area at level 3
ISO4	pixel <sup>2</sup>	1I	Isophotal area at level 4
ISO5	pixel <sup>2</sup>	1I	Isophotal area at level 5
ISO6	pixel <sup>2</sup>	1I	Isophotal area at level 6

ISO7	pixel <sup>2</sup>	1I	Isophotal area at level 7
ALPHA_J2000	deg	1D	SExtractor centroid right ascension (J2000)
DELTA_J2000	deg	1D	SExtractor centroid declination (J2000)
SG2DPHOT		1I	2DPhot StarGalaxy classifier (1 for high confidence star)
HTM		1J	Hierarchical Triangular Mesh (level 25)
FIELD_POS		1I	Reference number to field parameters
<b>List-driven GAAP photometry on the AstroWISE co-added KiDS images and the pawprint VIKING images:</b>			
Agaper_0p7	arcsec	1E	Major axis of GAaP aperture MIN_APER 0.7
Bgaper_0p7	arcsec	1E	Minor axis of GAaP aperture MIN_APER 0.7
Agaper_1p0	arcsec	1E	Major axis of GAaP aperture MIN_APER 1.0
Bgaper_1p0	arcsec	1E	Minor axis of GAaP aperture MIN_APER 1.0
PAgaap	deg	1E	Position angle of major axis of GAaP aperture (North of West)
<i>and then for each band <math>x \in \{u, g, r, i1, i2, Z, Y, J, H, Ks\}</math></i>			
FLUX_GAAP_0p7_x	Jy	1E	GAaP flux in band x with MIN_APER =0.7
FLUXERR_GAAP_0p7_x	Jy	1E	Error on FLUX_GAAP_0p7_x
MAG_GAAP_0p7_x	mag	1E	x-band GAaP magnitude with MIN_APER =0.7
MAGERR_GAAP_0p7_x	mag	1E	Error on MAG_GAAP_0p7_x
FLAG_GAAP_0p7_x		1J	GAaP Flag for x-band photometry with MIN_APER =0.7
FLUX_GAAP_1p0_x	Jy	1E	GAaP flux in band x with MIN_APER =1.0
FLUXERR_GAAP_1p0_x	Jy	1E	Error on FLUX_GAAP_1p0_x
MAG_GAAP_1p0_x	mag	1E	x-band GAaP magnitude with MIN_APER =1.0
MAGERR_GAAP_1p0_x	mag	1E	Error on MAG_GAAP_1p0_x
FLAG_GAAP_1p0_x		1J	GAaP Flag for x-band photometry with MIN_APER =1.0
<b>Optimal-aperture GAaP 10-band photometry including interstellar extinction corrections</b>			
Agaper	arcsec	1E	Major axis of GAaP aperture for optimal MIN_APER
Bgaper	arcsec	1E	Minor axis of GAaP aperture for optimal MIN_APER
<i>and then for each band <math>x \in \{u, g, r, i1, i2, Z, Y, J, H, Ks\}</math></i>			
EXTINCTION_x	mag	1E	Galactic extinction in band x
MAG_GAAP_x	mag	1E	Corrected x-band GAaP magnitude with optimal MIN_APER
MAGERR_GAAP_x	mag	1E	Error on MAG_GAAP_x
FLUX_GAAP_x	Jy	1E	x-band GAaP flux with optimal MIN_APER
FLUXERR_GAAP_x	Jy	1E	Error on FLUX_GAAP_x
FLAG_GAAP_x		1I	GAaP Flag for x-band photometry with optimal MIN_APER
MAG_LIM_x	mag	1E	x-band limiting magnitude for optimal MIN_APER
<b>10-band photometric redshifts (BPZ)</b>			
Z_B		1D	10-band BPZ redshift estimate (posterior mode)
Z_B_MIN		1D	Lower bound of the 68% confidence interval of Z_B
Z_B_MAX		1D	Upper bound of the 68% confidence interval of Z_B
T_B		1D	Spectral type corresponding to Z_B
ODDS		1D	Empirical ODDS of Z_B
Z_ML		1D	10-band BPZ maximum likelihood redshift
T_ML		1D	Spectral type corresponding to Z_ML
CHI_SQUARED_BPZ		1D	chi squared value associated with Z_B
M_0	mag	1D	Reference magnitude for BPZ prior

BPZ_FILTER		1J	filters with good photometry (BPZ)
NBPZ_FILTER		1J	number of filters with good photometry (BPZ)
BPZ_NONDEFILTER		1J	filters with faint photometry (BPZ)
NBPZ_NONDEFILTER		1J	number of filters with faint photometry (BPZ)
BPZ_FLAGFILTER		1J	flagged filters (BPZ)
NBPZ_FLAGFILTER		1J	number of flagged filters (BPZ)
SG_FLAG		1E	Star/Gal Classifier
MASK		1J	10-band mask information
<b>PSF estimates (<i>lensfit</i>)</b>			
PSF_e1		1E	mean ellipticity of PSF, component 1
PSF_e2		1E	mean ellipticity of PSF, component 2
PSF_Strehl_ratio		1E	Pseudo-Strehl ratio of PSF
PSF_Q11		1E	model PSF moment Q11
PSF_Q22		1E	model PSF moment Q22
PSF_Q21		1E	model PSF moment Q21
<b>Stellar Mass estimates (LePhare)</b>			
<i>for each band <math>x \in \{u, g, r, i1, i2, Z, Y, J, H, Ks\}</math></i>			
MAGABS_GAAP_x		1D	rest-frame x-band magnitude
KCOR_x		1D	x-band k-correction
LUM_GAAP_r_bestfit		1D	r-band luminosity
mstar_bestfit		1D	stellar mass
mstar_med		1D	posterior median stellar mass
mstar_lower		1D	posterior 16 <sup>th</sup> percentile stellar mass
mstar_upper		1D	posterior 84 <sup>th</sup> percentile stellar mass
sfr_bestfit		1D	star-formation rate
sfr_med		1D	posterior median star-formation rate
sfr_lower		1D	posterior 16 <sup>th</sup> percentile star-formation
sfr_upper		1D	posterior 84 <sup>th</sup> percentile star-formation
<b>THELI Astrometry Error Flags</b>			
max_dRADec_AW	deg	1D	Max separation between THELI and AW coadd
max_dRADec_THELI	deg	1D	Max internal separation exposure centroid and stack
ast_flag		1B	Fiducial astrometric accuracy selection
<b>Dereddened colours based on optimal-aperture GAAP photometry</b>			
COLOUR_GAAP_u_g	mag	1E	u-g colour index (dereddened)
COLOUR_GAAP_g_r	mag	1E	g-r colour index (dereddened)
COLOUR_GAAP_r_i1	mag	1E	r-i_1 colour index (dereddened)
COLOUR_GAAP_r_i2	mag	1E	r-i_2 colour index (dereddened)
COLOUR_GAAP_i1_Z	mag	1E	i_1-Z colour index (dereddened)
COLOUR_GAAP_i2_Z	mag	1E	i_2-Z colour index (dereddened)
COLOUR_GAAP_Z_Y	mag	1E	Z-Y colour index (dereddened)
COLOUR_GAAP_Y_J	mag	1E	Y-J colour index (dereddened)
COLOUR_GAAP_J_H	mag	1E	J-H colour index (dereddened)
COLOUR_GAAP_H_Ks	mag	1E	H-K_s colour index (dereddened)
DIFF_GAAP_i1_i2	mag	1E	i_1-i_2 i-band magnitude difference

## Acknowledgements

Users of data from this release should cite "Wright et al. (2024, A&A, 686, 170)".

According to the Data Access Policy for ESO data held in the ESO Science Archive Facility, all users are required to acknowledge the source of the data with appropriate citation in their publications. Since processed data downloaded from the ESO Archive are assigned Digital Object Identifiers (DOIs), the following statement must be included in all publications making use of them:

- *Based on data obtained from the ESO Science Archive Facility with DOI: <https://doi.org/10.18727/archive/37>, and <https://doi.eso.org/10.18727/archive/59> and on data products produced by the KiDS consortium. The KiDS production team acknowledges support from: Deutsche Forschungsgemeinschaft, ERC, NOVA and NWO-M grants; Target; the University of Padova, and the University Federico II (Naples).*

Publications making use of data which have been assigned an archive request number (of the form XXXXXX) must also include the following statement in a footnote or in the acknowledgement:

- *Based on data obtained from the ESO Science Archive Facility under request number <request\_number>.*

Science data products from the ESO archive may be distributed by third parties, and disseminated via other services, according to the terms of the [Creative Commons Attribution 4.0 International license](#). Credit to the ESO provenance of the data must be acknowledged, and the file headers preserved.